Formic acid dehydrogenation reaction on high-performance Pd_xAu_{1-x} alloy nanoparticles prepared by the eco-friendly slow synthesis methodology

Yibo Gao[a], Erjiang Hu[a,*], Bo Huang[b,*], Zuohua Huang[a]

[a] State Key Laboratory of Multiphase Flow in Power Engineering, Xi'an Jiaotong University, Xi'an 710049, China.

[b] Institute of Chemical Engineering and Technology, Xi'an Jiaotong University, Innovation Harbour, Xi'an 712000, China.

Corresponding author：

Erjiang Hu

State Key Laboratory of Multiphase Flow in Power Engineering,

Xi'an Jiaotong University, Xi'an 710049, China.

E-mail: hujiang@mail.xjtu.edu.cn (Erjiang Hu).

Bo Huang

Institute of Chemical Engineering and Technology, Xi'an Jiaotong University, Innovation Harbour, Xi'an 712000, China.

E-mail: bohuang@mail.xjtu.edu.cn (Bo Huang).

1. Reduction Potentials of Noble Metals

Table S1. Reduction Potentials of the Noble Metals Under Standard Conditions (25 °C, 1 atm).

SHE: Standard Hydrogen Electrode

Reduction reaction	***E*°(V vs SHE)**
$Pd^{2+} + 2e^- \rightarrow Pd$	0.951
$Au^{3+} + 3e^- \rightarrow Au$	1.498
$Ru^{2+} + 2e^- \rightarrow Ru$	0.455
$Ag^{+} + e^- \rightarrow Ag$	0.800
$Ir^{3+} + 3e^- \rightarrow Ir$	1.156
$Pt^{2+} + 2e^- \rightarrow Pt$	1.188

2. Metal Compositions of Pd_xAu_{1-x} NPs

Table S2. Metal compositions of Pd_xAu_{1-x} alloy NPs determined from ICP-MS and EDX analysis.

Sample	Pd:Au (nominal composition)	Pd:Au (determined from ICP-MS)	Pd:Au (determined from EDX)
$Pd_{0.2}Au_{0.8}$	20 : 80	18.7 : 81.3	19.5 : 80.5
$Pd_{0.4}Au_{0.6}$	40 : 60	36.4 : 63.6	41.4 : 58.6
$Pd_{0.5}Au_{0.5}$	50 : 50	52.7 : 47.3	49.3 : 50.7
$Pd_{0.6}Au_{0.4}$	60 : 40	64.1 : 35.9	62.3 : 37.7
$Pd_{0.8}Au_{0.2}$	80 : 20	81.3 : 18.7	77.6 : 22.4

3. HAADF-STEM images of Pd_xAu_{1-x} (x = 0, 0.4, 0.6 and 1) NPs

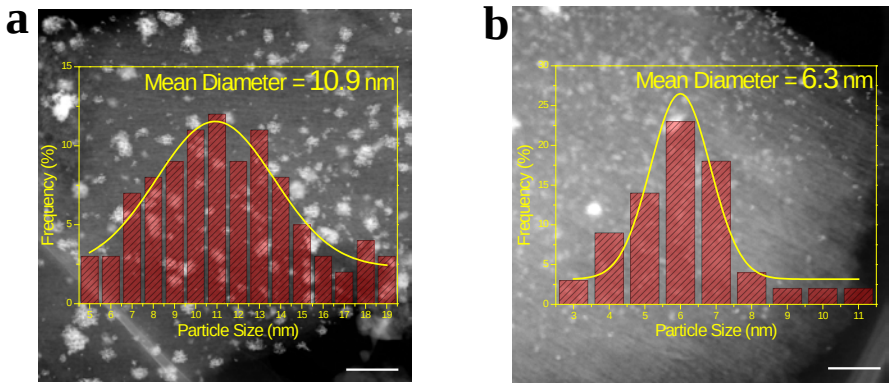

Fig. S1. High-angle annular dark-field scanning transmission electron microscopy (HAADF-STEM) images of (a) Au NPs and (b) Pd NPs. All scale bars are 20 nm.

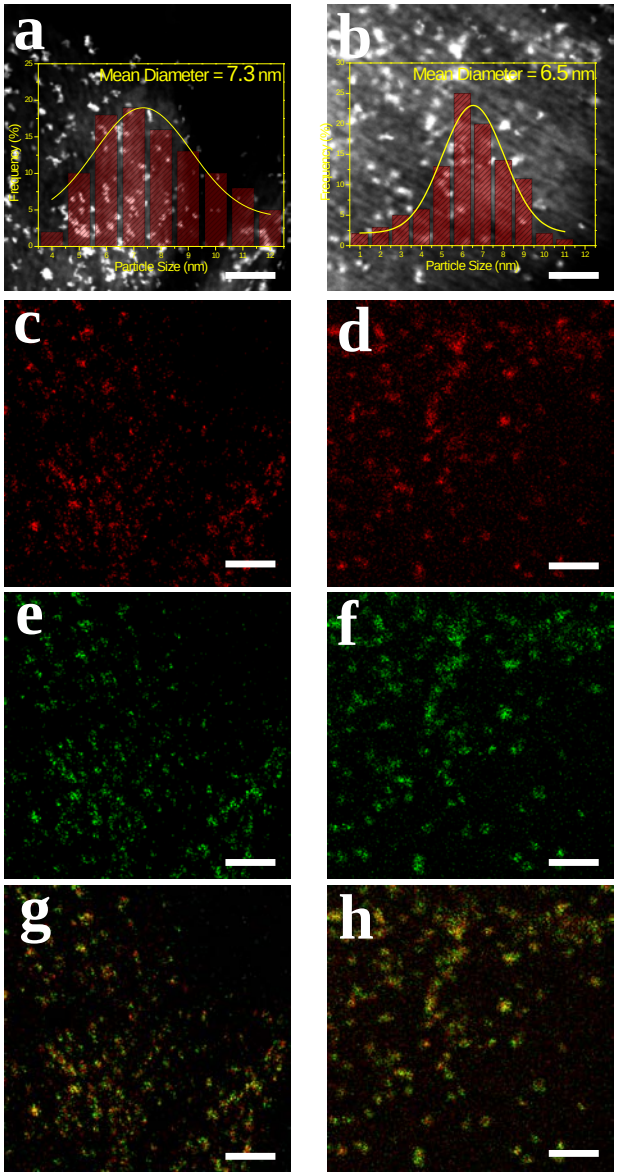

Fig. S2. High-angle annular dark-field scanning transmission electron microscopy (HAADF-STEM) images of (a) $Pd_{0.4}Au_{0.6}$ and (b) $Pd_{0.6}Au_{0.4}$. (c)-(d), (e)-(f) and (g)-(h) are the corresponding Pd-L, Au-L and overlay images STEM energy-dispersive X-ray (EDX) maps of (a)-(b). All scale bars are 50 nm.

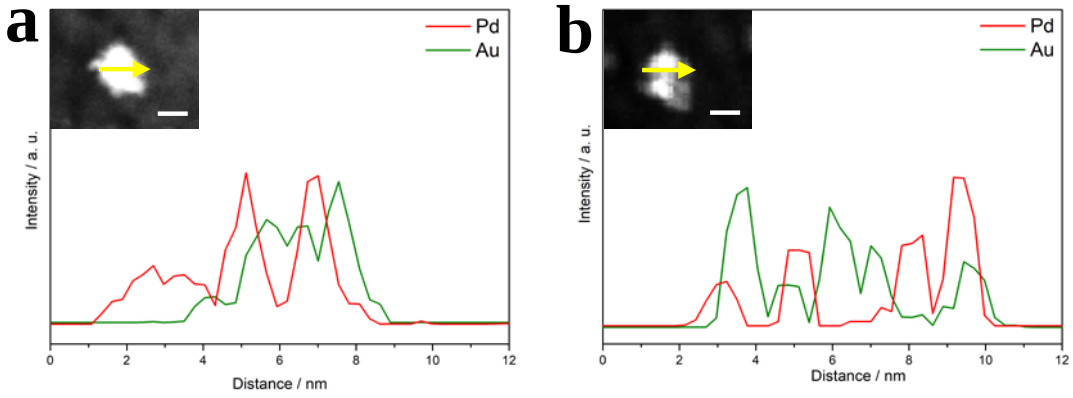

Fig. S3. EDX line profiles of the NPs along the arrows shown in inset figures of (a) $Pd_{0.4}Au_{0.6}$ and (b) $Pd_{0.6}Au_{0.4}$ NPs. Pd and Au are indicated in red and green colors, respectively. The scale bars shown in (a) and (b) are 10 nm.

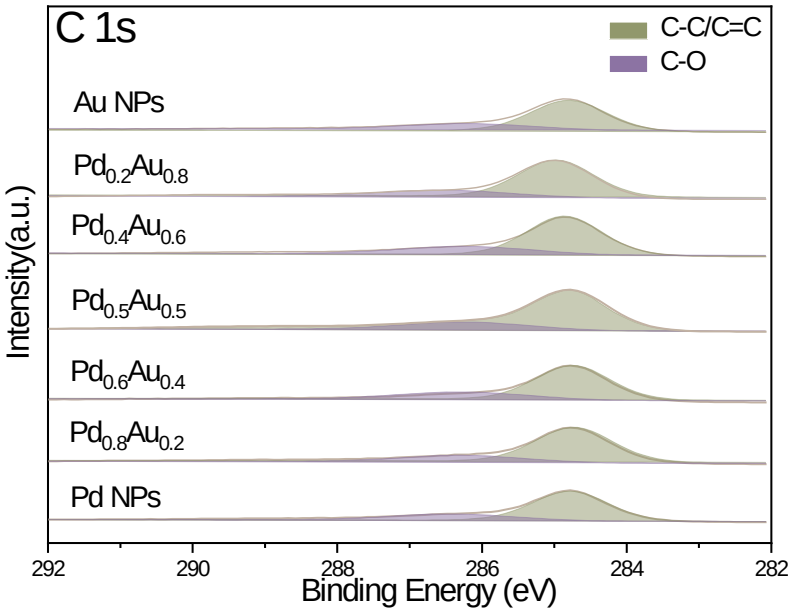

Fig. S4. XPS spectra of C 1s in the Pd_xAu_{1-x} (x = 0, 0.2, 0.4, 0.5, 0.6, 0.8, 1) alloy NPs.

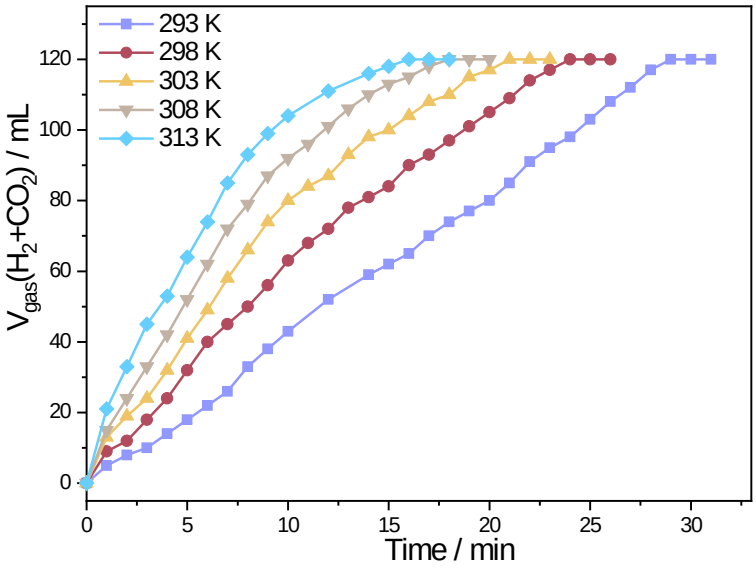

Fig. S5. Generated $V_{(H_2+CO_2)}$ versus time for the dehydrogenation of FA in FA-SF aqueous solution over $Pd_{0.5}Au_{0.5}$ at different reaction temperatures (n_{Pd+Au}/n_{FA} = 0.01, n_{FA}/n_{SF} = 1:3).

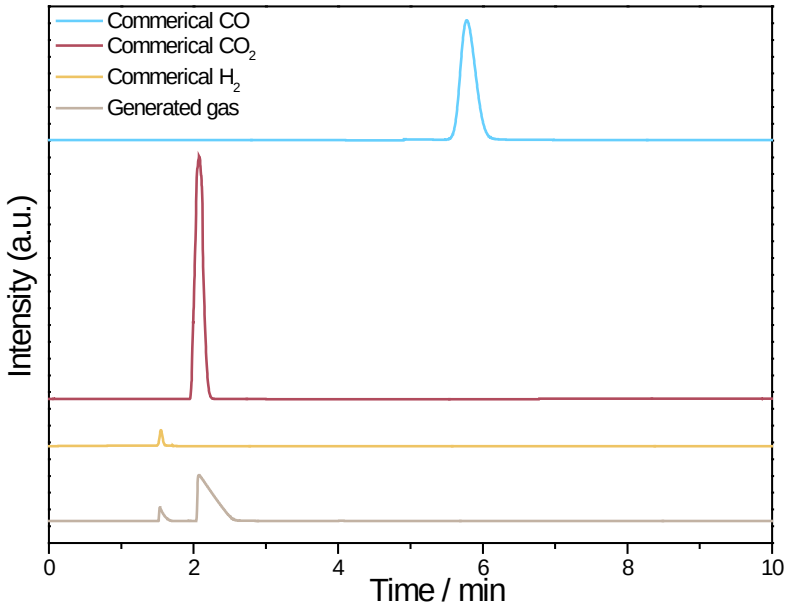

Fig. S6. Gas chromatogram of CO_2, CO and H_2 as reference gases and the generated gases from aqueous FA/SF solution over the $Pd_{0.5}Au_{0.5}$ (313 K, n_{Pd+Au}/n_{FA} = 0.01, n_{FA}/n_{SF} = 1:3).

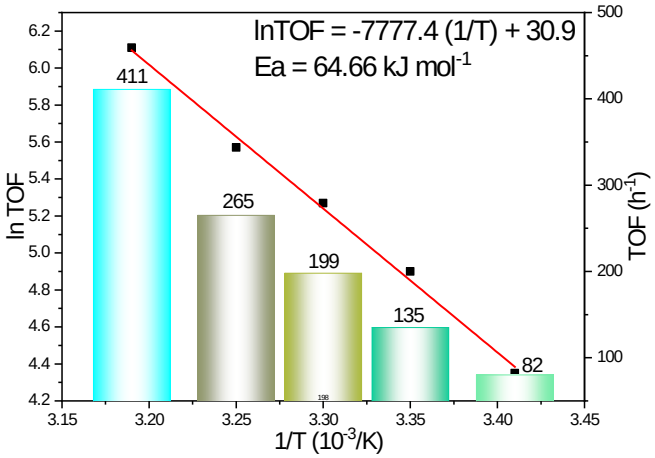

Fig. S7. Arrhenius plot and corresponding kinetic parameters over Pd NPs catalyst.